# Idealized Numerical Modeling of a Land/Sea Breeze

Jeremy A. Gibbs

School of Meteorology, University of Oklahoma

3 December 2008

## 1 Introduction

With references in the Bible, the land and sea breeze is one of the oldest studied meteorological phenomena. Neumann (1973) noted that Aritotle discussed sea breezes in his *Problemata*:

> *Why do the alternating winds blow? Is it for the same reason as causes the change in current in straits? For both sea and air are carried along until they flow; then, when the land-winds encounter opposition and can no longer advance, because the source of their motion and impetus is not strong, they retire in a contrary direction.*

Further inclusion in the literature includes that from Halley (1686). Despite this long history, the traditional "convectional" theory of the land sea breeze remains quite pertinent. This theory, as stated in Buchan (1860), stipulates that the land and sea breeze is caused when land is “heated to a much greater degree than the sea during the day, by which air resting on it being also heated, ascends, and the cooler air of the sea breeze flows in to supply its place. But during the night the temperature of the land and the air above it falls below that of the sea, and the air thus becoming heavier and denser flows over the sea as a land breeze.”

This paper offers a brief overview of linear theory of the land and sea breeze as described in Rotunno (1983). Idealized numerical modeling of the land and sea breeze is then offered in an attempt to reproduce the structure of the breeze when $f < \omega$, in which the atmospheric response is in the form of internal gravity waves. Additionally, the effects of land expanse and model grid spacing is investigated and discussed.

## 2 Linear Theory of the Land and Sea Breeze

Rotunno (1983) outlines the so-called linear theory of the land and sea breeze. The Boussinesq equations are first linearized and made two-dimensional by setting $\frac{\partial}{\partial y} = 0$. This results in the following set of equations of motion,

$$\frac{\partial u'}{\partial t} - fv = -\frac{\partial \Pi'}{\partial x} + F^x \ , \tag{1}$$

$$\frac{\partial v'}{\partial t} + fu = +F^y \ , \tag{2}$$

$$\frac{\partial w'}{\partial t} - B = -\frac{\partial \Pi'}{\partial z} + F^z \ , \tag{3}$$

$$\frac{\partial b}{\partial t} + N^2 w' = Q \ , \tag{4}$$

$$\frac{\partial u'}{\partial x} + \frac{\partial w'}{\partial z} = 0 \ , \tag{5}$$

where $u, v$, and $w$ are component of velocity in the $x, y$, and $z$ directions, respectively.

$$\Pi = c_p\theta_o \left(\frac{P}{P_o}\right)^{\frac{R}{c_p}} ,$$

where $P, P_o, R, c_p$ and $N$ are the pressure, surface pressure, gas constant for air, specific heat at constant pressure, and the Brunt-Väisälä frequency. The lower boundary is $w(x, o, t) = 0$. Other boundary conditions may exist depending on $F^{x,y,z}$.

The quantities $v', B$, and $\Pi'$ are eliminated in order to form two equations

$$u' = \frac{\partial\psi}{\partial z} \quad \text{and} \tag{6}$$

$$v' = -\frac{\partial\psi}{\partial x} . \tag{7}$$

Next, a vorticity equation is formed, taking $Q \sim e^{-i\omega t}$ and $\psi \sim e^{-i\omega t}$, and assuming $N^2 \gg \omega^2$

$$N^2 \frac{\partial^2\psi}{\partial x\partial x} + \left(f^2 - \omega^2\right) \frac{\partial^2\psi}{\partial z\partial z} = -\frac{\partial Q}{\partial x} . \tag{8}$$

Here, $(f^2 - \omega^2)$ is important, because depending on whether the term is positive or negative, one will arrive at one of three differing solutions:

1. $f > \omega$. solution is elliptic and and the forcing response is confined locally,

2. $f < \omega$. solution is hyperbolic and the forcing response is in the form of internal gravity waves.

3. $f = \omega$. solution is singular and friction must be included.

This paper focuses on the hyperbolic solution, where $f < \omega$.

# 3 The Model

One of the more popular state-of-the-art NWP models is The Weather Research and Forecasting (WRF) model (Skamarock et al. 2008). The WRF model is a is a highly portable code that can run on a wide range of computing platforms, including both desktop environments and multi-processor supercomputing clusters. The model includes two dynamical solvers, numerous physical parameterization packages, an intricate initialization program, and an advanced three-dimensional variational (3DVAR) data assimilation system. For this study, WRF version 3.0.1 was employed utilizing the Advanced Research WRF (ARW) dynamical core. The ARW solves Euler non-hydrostatic, fully-compressible governing equations of atmospheric dynamics and thermodynamics utilizing the staggered Arakawa C-grid and vertical $\eta$-coordinate.

This study took advantage of the model's built in idealized solver. Instead of initializing the model with real data from gridded analyses, the user prescribed an ideal set of atmospheric paramters suitable for the desired phenomena. This is generally done by creating an idealized sounding of meteorological quantities along with forcing the background environment to a suitable one for the respective simulation. The ability to run ideal cases allows the user to gain a physical understanding of the phenomena itself by only considering the most basic and necessery paramaters required to reproduce the appropriate feature. Essentially, this allows one to remove as much clutter as possible to better understand the features of the considered case.

# 4 Model Run Arrangements

For these experiments, a two-dimensional (x-z plane) land and sea breeze was modeled. A simulation domain spanning 400km × 20km was employed with varying horizontal grid spacing. Periodic lateral boundary conditions were employed. The elevation was taken as 0m ASL. Variable horizontal extent of land was explored. The land was centered in the domain, leaving water on either side. The central latitude and longitude were taken as the intersection of the prime meridian and the equator. This allowed for coriolis to be omitted. The simulation window covered a 24h timeframe beginning at 06UTC. Note that since the domain is centered on the prime meridian, 06UTC, corresponds to 6A.M. local time. This allowed for a clear picture of the diurnal pattern of the land and sea breeze. Full physics were employed, using the WRF single moment 3-class microphysics scheme, the Dudhia and RRTM radiation schemes, the Noah land-surface model, the MM5/YSU surface-layer/PBL combination for vertical diffusion, and a two-dimensional Smagorinsky closure for horizontal diffusion. Initially, the ocean surface temperature was set as 7K larger than that of the land surface temperature. Table (1) lists the different model configurations used in modeling the land and sea breeze.

# 5 Results

As the simulation window began, there was initally zero wind and the ocean was 7K warmer than the land surface temperature. Nothing occured until several hours passed, as heating of the land began. By 11UTC, baroclinically generated vorticity was created on the land/sea

Table 1: Configurations for WRF model runs

| **DX** | **Land Extent** | **Abbrev** |
|---|---|---|
| 2km | 100km | LSB2-100 |
| 2km | 200km | LSB2-200 |
| 2km | 40km | LSB2-40 |
| 1km | 100km | LSB1-100 |
| 500m | 100km | LSB500-100 |

interfaces, as seen in Figure (1). For all images, the upper left panel depicts u-component velocity ($ms^{-1}$), the upper right panel depicts w-component velocity ($ms^{-1}$), the lower left plot depicts perturbation pressure (hPa), and the lower right panel depicts potential temperature (K). An onshore component of horizontal velocity coincided with this vorticity. At the same time, pressure thickness on land increased as negative pressure perturbations were created over land and positive perturbations over water existed. Cooler temperatures from over water began advecting onshore.

As the day progressed, by 16UTC, the flow on either side of the land continued to propogate onshore until converging in the center of the land mass. At this point, the vertical velocity was at its largest value, as was the offshore positive pressure perturbations and the actual land sea breeze itself. The return flow aloft was evident at this point in the simulation window, as were the intertial gravity waves emanating from the main forcing in the center of the domain. This is illustrated in Figure (2).

By 21UTC, as daytime heating had ceased and the ground began cooling, the land and sea breeze became weaker and more shallow. The internal gravity waves were clearly present when looking at the u-component velocity. Pressure perturbations became positive over land and negative over water, as the flow began to switch from a sea breeze to a land breeze. Vertical velocity coincided with offshore forcing. This behavior is seen in Figure (3).

During nightime (02UTC), the forcing was weak and the flow was predominantly a land breeze, which was small in magnitude when compared to the sea breeze. Pressure perturbations were very small as was the vertical velocity. Accordingly, the potential temperature field remained fairly uniform in the horizontal. The land breeze is demonstrated in Figure (4).

When comparing differing resolutions, solutions remained fairly close. However, as the grid spacing decreased, the respective forcings were represented as stronger. For example, as seen in Figures (5) and (6), the perturbations of prssure along with vertical velocity and the land and sea breeze were stronger in the LSB500-100 than any other case. This is likely a result of better resolved turbulence surface interactions than in a coarser grid. Additionally, using a PBL scheme at 500m grid spacing may lead to an additive effect that overestimates each respective forcing.

When comapring with differing spatial extent of land, it is clear than the magnitude of each forcing is highly dependent of the span of the land. For instance, looking at Figure (7), a land extent twice as large, results in larger predictions of vertical velocity, pressure perturbations, and the actual onshore component of the wind. Conversely, the smaller land span resulted in smaller land and sea breeze, as seen iin Figure (8). This behavior is likely dependent on the distance for each disturbance to travel, as well as the actual fetch of land available for heating.

# 6 Summary

Rotunno (1983) describes linear theory for the land and sea breeze when $f < \omega$. This results in a hyperbolic solution whose response is in the form of internal gravity waves. The WRF model, run in idealized mode, was able to reproduce the expected results given an initial temperature difference between land and sea of 7K. The onshore sea breeze was illustrated during the day and the land breeze during the nighttime. Varying the horizontal grid spacing would result in different forcing, specifically, larger forcing for smaller grid spacings. This may be a result of increased resolvable scales, or an additive effect from using a PBL scheme at finer resolutions. Changing the fetch of land greatly impacted the behavior of the land and sea breeze. The longer the span, the more heating could occur in the center while the onshore components propogated inland. This resulted in a much stronger land and sea breeze. Overall, it appears that the WRF model adequately reproduced the expected structure and bahavior of the land and sea breeze as described Rotunno (1983).

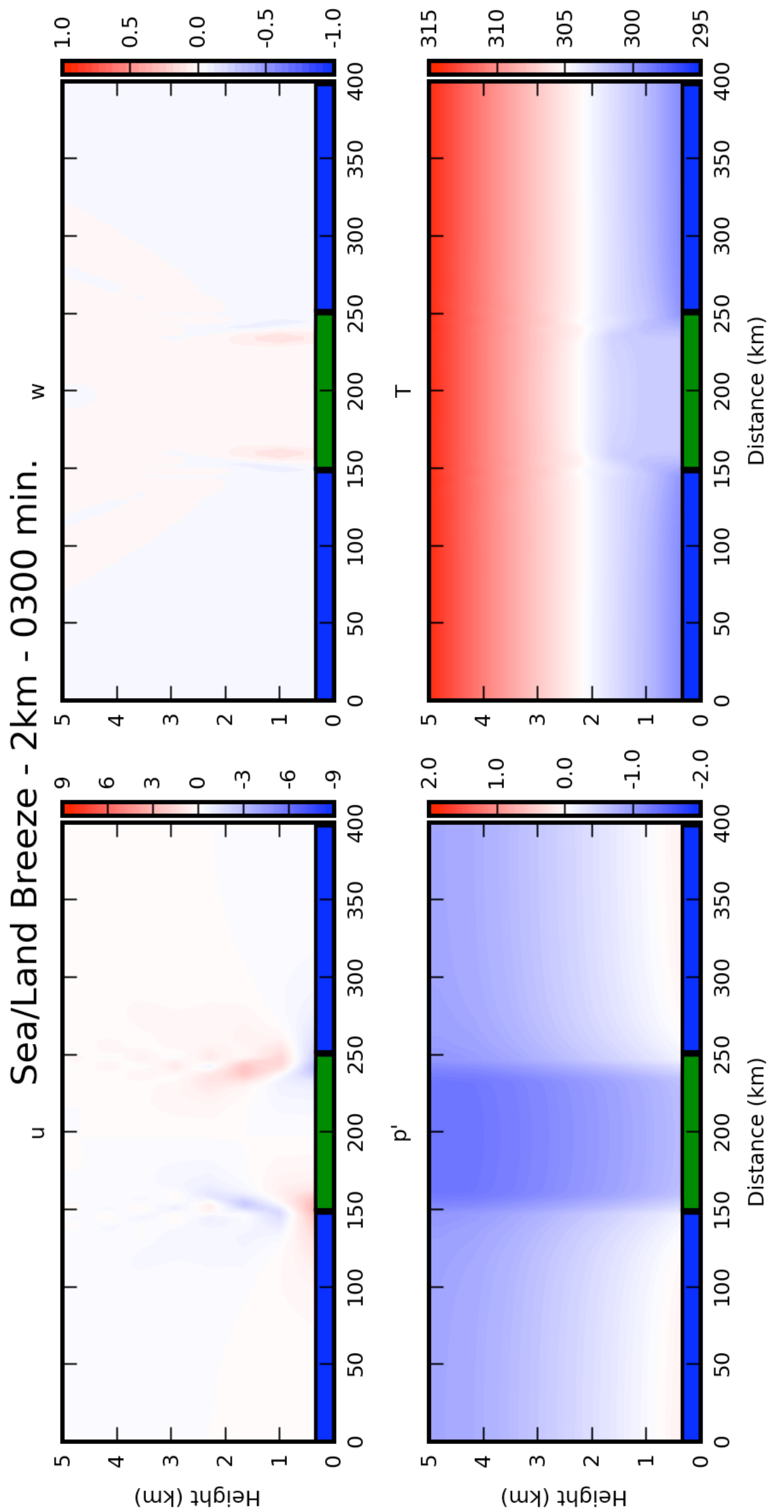


Figure 1: Land and sea breeze evolution at 11UTC for LSB200-100.

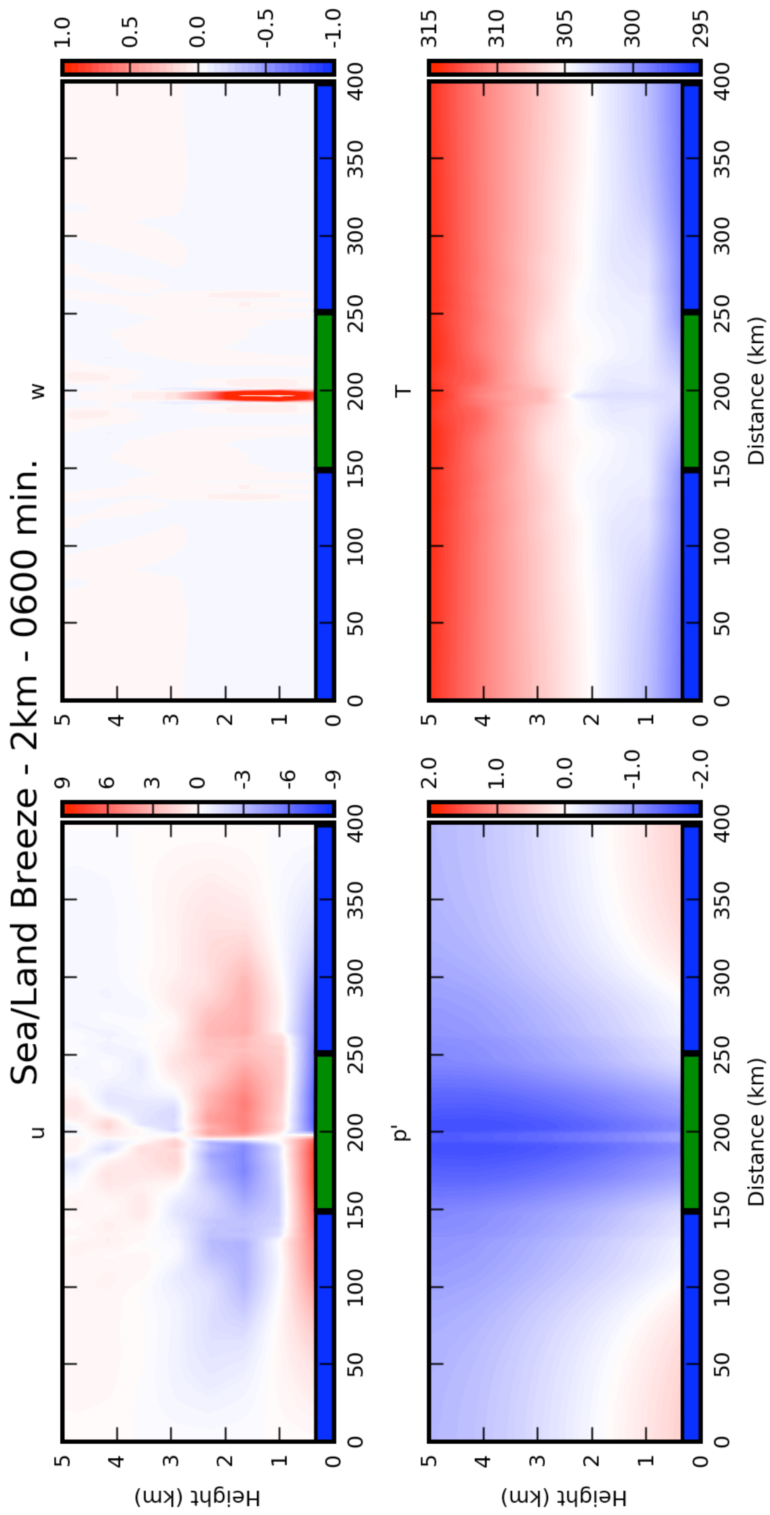


Figure 2: Land and sea breeze evolution at 16UTC for LSB2-100.

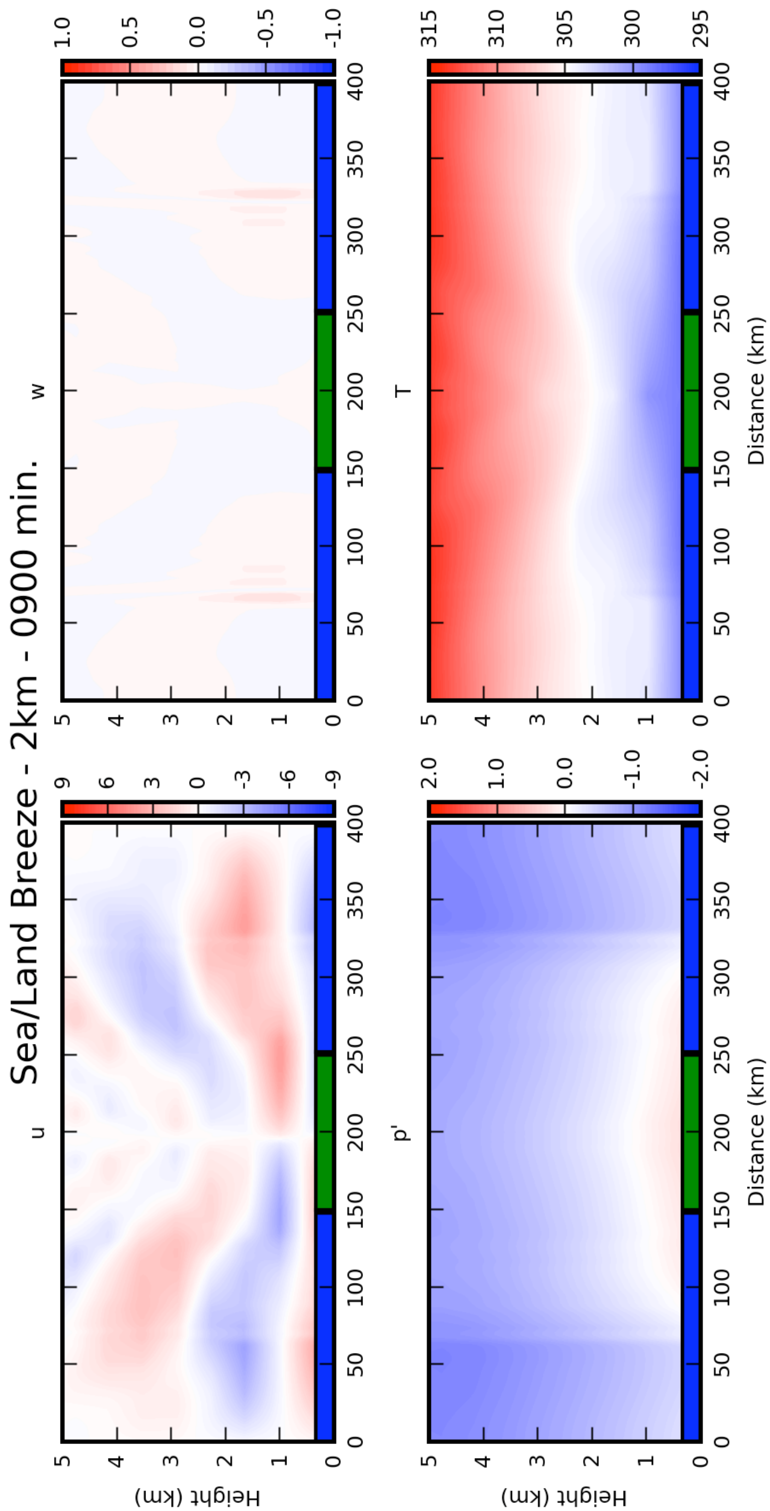


Figure 3: Land and sea breeze evolution at 21UTC for LSB2-100.

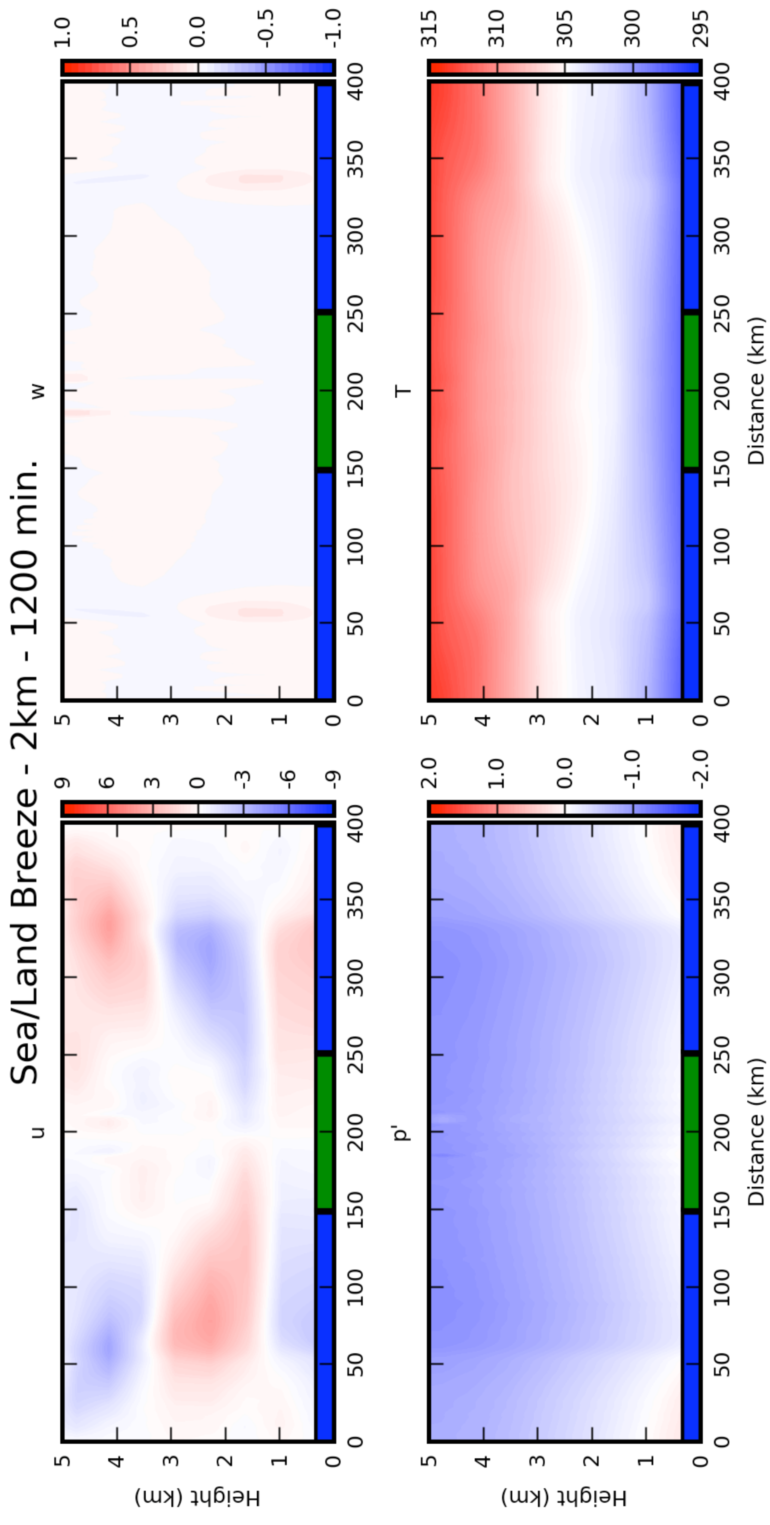


Figure 4: Land and sea breeze evolution at 02UTC for LSB2-100.

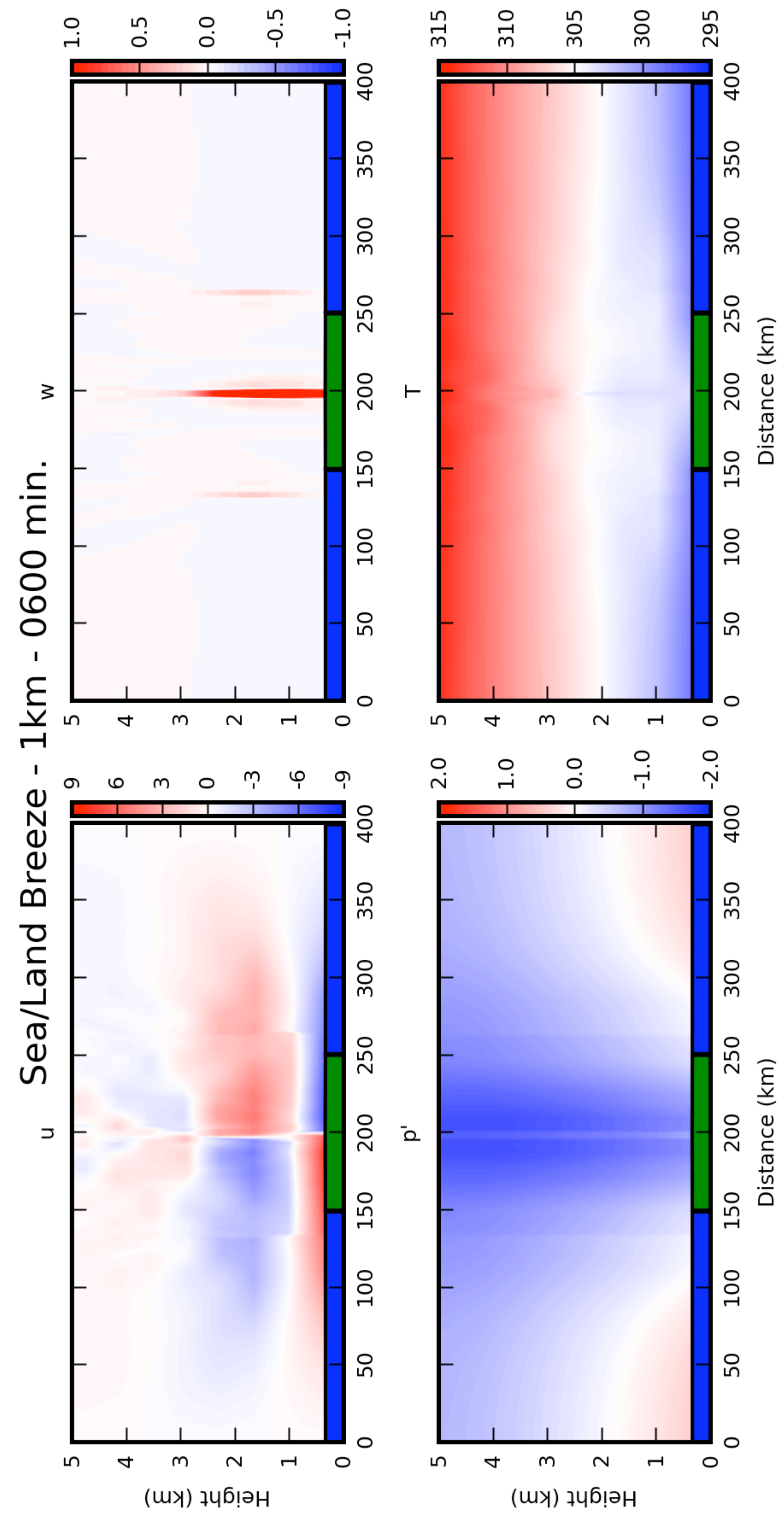


Figure 5: Land and sea breeze evolution at 16UTC for LSB1-100.

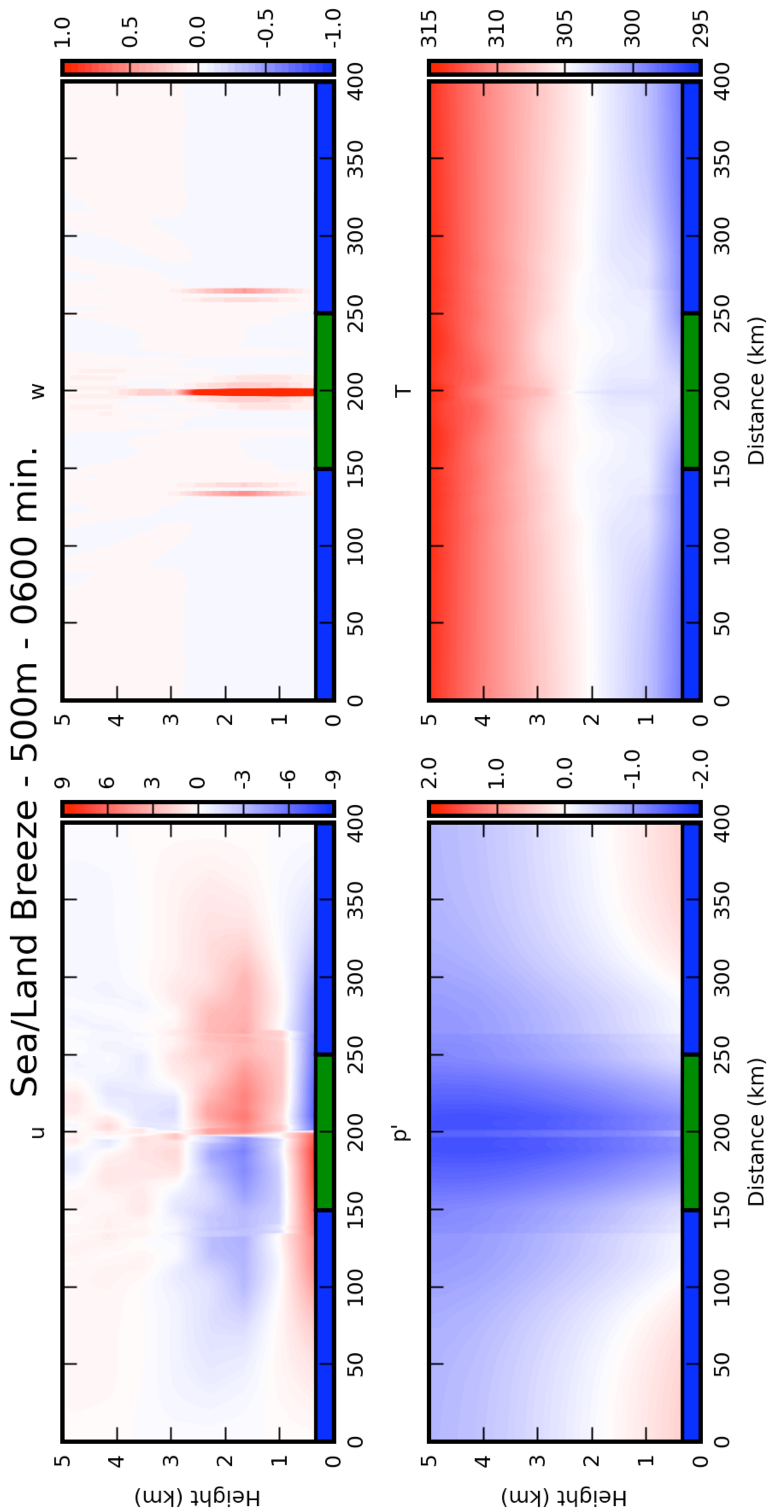


Figure 6: Land and sea breeze evolution at 16UTC for LSB500-100.

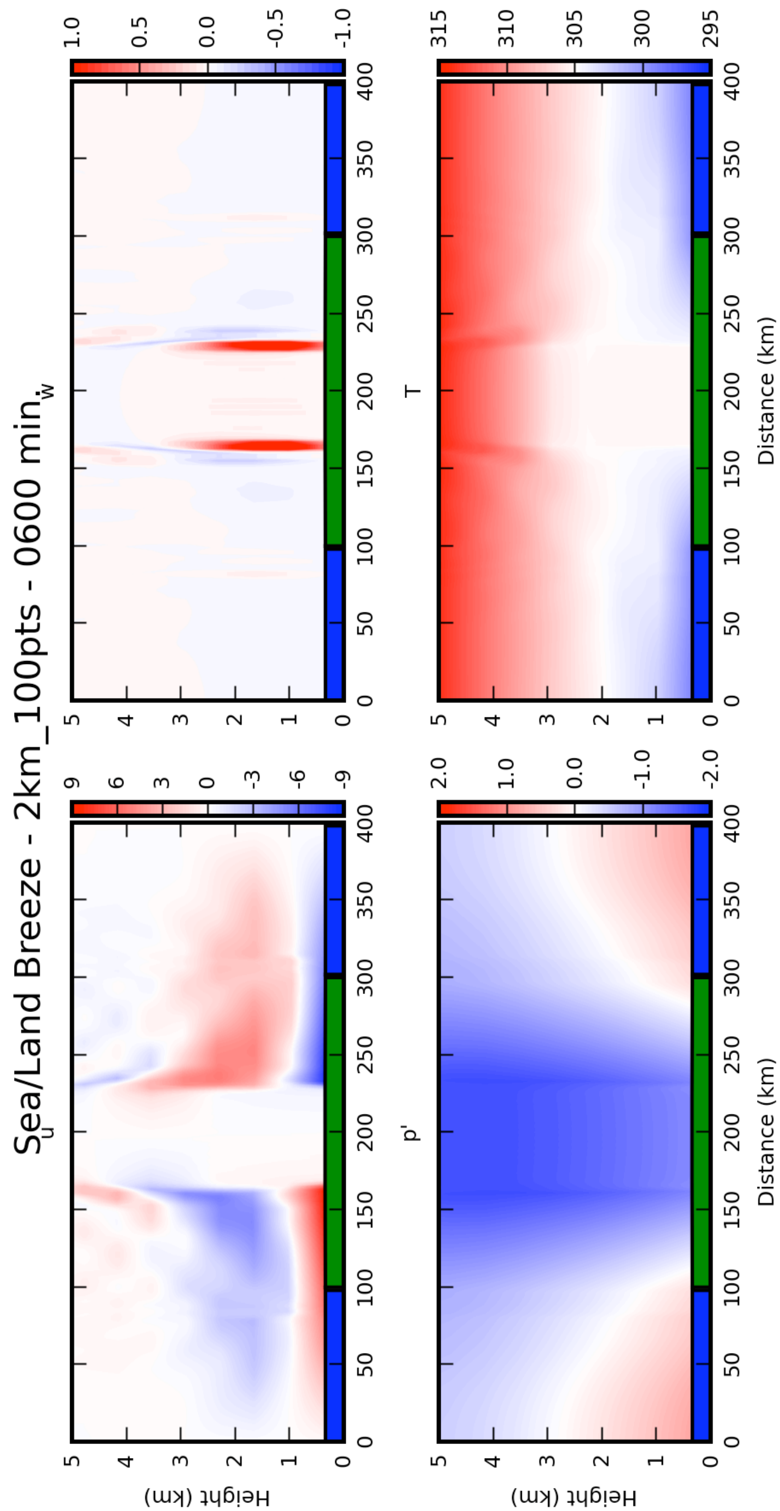


Figure 7: Land and sea breeze evolution at 16UTC for LSB2-200.

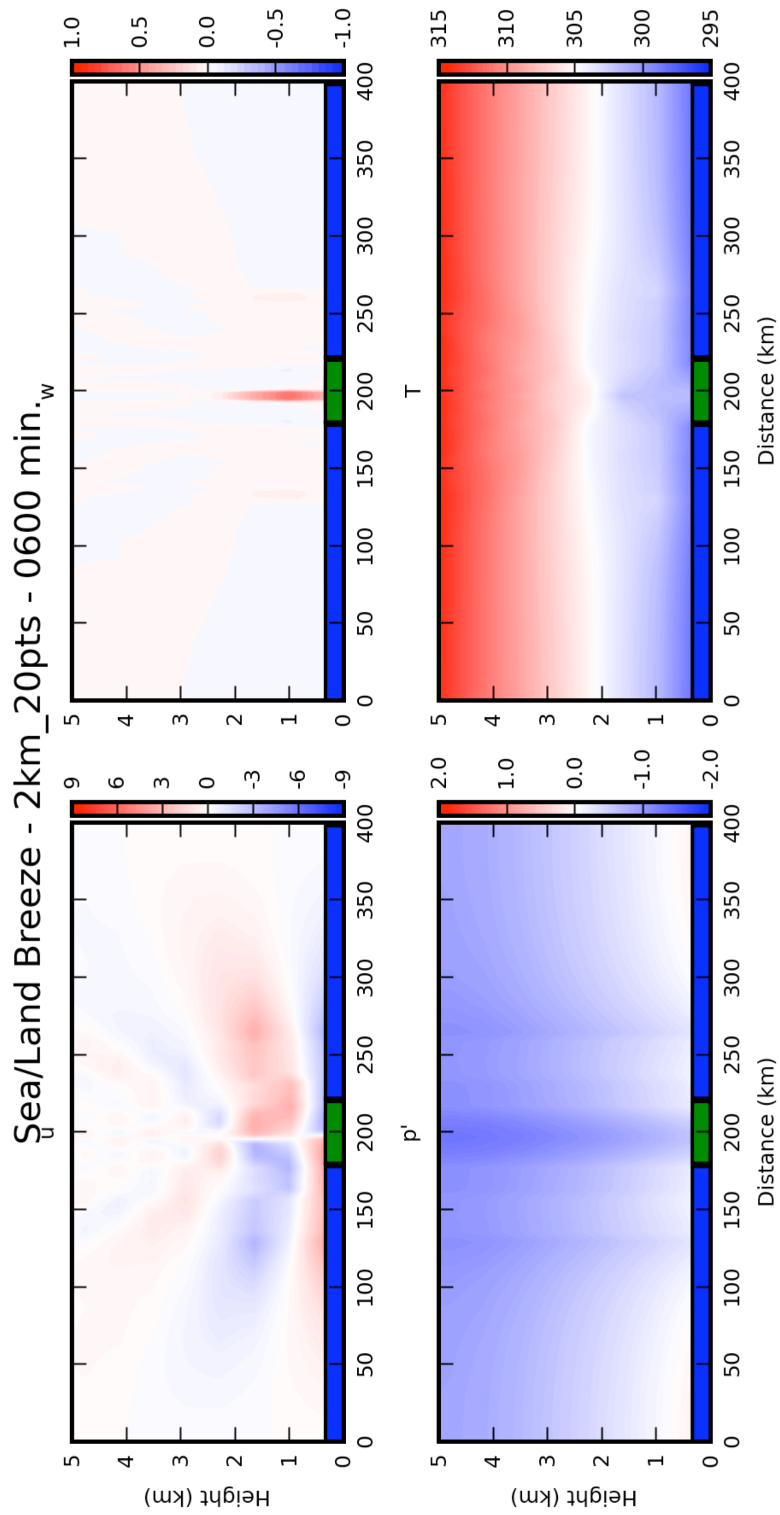


Figure 8: Land and sea breeze evolution at 16UTC for LSB2-40.

## References


Buchan, A., 1860: *Handy Book of Meteorlogy*. Blackwood and Sons, New York, 371 pp.

Halley, E., 1686: An historical account of the trade winds, and monsoons, observable in the seas between and near the tropicks, with an attempt to assign physical cause of said winds. *Phil. Trans. Roy. Soc. London*, **16**, 153–168.

Neumann, 1973: The Sea and Land Breezes in the Classical Greek Literature. *Bull. Amer. Meteor. Soc.*, **55**, 5–8.

Rotunno, R., 1983: On the Linear Theory of the Land and Sea Breeze. *J. Atmos. Sci.*, **40**, 1999–2009.

Skamarock, W. C., J. B. Klemp, J. Dudhia, D. O. Gill, D. M. Barker, W. Wang, and J. G. Powers, 2008: A Description of the Advanced Research WRF Version 3. Technical report, NCAR, USA.